ILASS–Europe 2022, 31th Conference on Liquid Atomization and Spray Systems, 6-8 September 2022, Virtual, Israel

Vortex And Cavitation Driven Liquid Fragmentation In High Pressure Gasoline Direct Injections

Junmei Shi*[1], Ramesh Venkatasubramanian[1], Eduardo Gomez Santos[1], Guy Hoffmann[1], Wolfgang Bauer[2]

[1]Advanced Gasoline Components – BorgWarner Luxembourg Automotive Systems, Avenue de Luxembourg 274, L-4940 Hautcharage, Luxembourg

[2]ANSYS Germany GmbH, Staudenfeldweg 20, 83624 Otterfing, Germany

*Corresponding author: jushi@borgwarner.com

Abstract

In a previous work the research group has demonstrated evidence of vortex driven atomization in high pressure diesel injection [1] [2] [3]. This paper presents an extension to the Gasoline Direct injection (GDi) atomization. The effect of vortex dynamics and cavitation in the nozzle flow on the liquid fragmentation of GDi spray was investigated using Scale-Resolved-Simulation (SRS) techniques. A homogeneous mixture model was employed for the description of the multiphase flow system consisting of n-heptane liquid, vapor and air. Cavitation is modelled by using an Equation of State of a Barotropic fluid [4]. Large Eddy Simulation (LES) in combination with a Coupled Level-Set and Volume of Fluid (CLSVOF) method was adopted to resolve turbulence and liquid-gas interfaces in the nozzle flow and in the primary breakup process. The results reveal that massive vortices and cavitation streams originate from the needle surface and at the spray hole inlet. These flow structures experience a sudden expansion in the downstream counter bore following the flow path geometry change, yielding multiple anti-rotating swirling vortices and massive cavitation. The cavitation vapor occurs in the core of fuel flow and extends up to 0.5mm~1mm downstream of the counter bore exit before being condensed. Breakup process begins inside the counter bore where the liquid core is immediately destroyed as a result of the flow expansion and massive cavitation. Links between liquid surface deformation in the counter bore and vortex structures in the upstream flow are also identified. In addition, the influence of the counter bore size and the injection pressure on the root spray will be presented.

Keywords

GDi, Primary Breakup, CLSVOF-LES, Vortex, Cavitation

Introduction

Very different GDi nozzle designs can be found in the market or from literature, e.g. convergent hole (length-to-diameter ratio $l/d < 1.5$) with a counter bore (also called step hole, a wider opening directly downstream of a spray hole and the direct interface to the combustion chamber), divergent hole ($l/d < 1.5$) with a counter bore, long convergent hole ($l/d > 2$) without a counter bore, and very long divergent hole ($l/d > 3$) without a counter bore. Therefore questions like the following are often raised in the advanced development: Does the counter bore play a real function in spray atomization? Or what is the suitable counter bore size? Which type of spray hole design is the best for a 500bar+ GDi system (which has been confirmed to significantly reduce gaseous and particulate emissions [5])? Other more generic questions are: How to reduce critical jet penetration? How to control spray stability? What design features can be introduced to minimize injector coking (deposit forming at the injector tip)? The present research was initiated to provide fundamental background knowledge to answer the above questions for the advanced GDi spray development. Large Eddy Simulation was carried out to resolve the turbulence and interface scales in the nozzle and near-nozzle spray in order to gain a detailed insight into the high pressure GDi spray formation process.

The simulation was realized using a commercial software ANSYS FLUENT. An User Defined Function (UDF) implementation of a Barotropic cavitation model [4] was introduced to ensure the cavitation modelling fidelity. The analysis has revealed that liquid fragmentation starts in the counter bore and the large scale vortices formed in the sac due to flow turning (streamline curvature) and cavitation play a major role in the GDi spray formation process. Implications of these findings on spray control and spray modelling are discussed. In addition, transfer functions (metrics) taking into account the kinetic energy of secondary flow in the spray hole and counter bore was developed for the spray penetration correlation.

The vortex flow and string cavitation phenomenon have gained increasing research interest recently. The link between vortex flow, string cavitation and spray dispersion in diesel injection might have been first demonstrated by [6] [7] through simultaneous visualization of nozzle flow cavitation and spray and recently investigated by [8] using both flow visualization and LES analysis. Numerical analysis of the turbulence and cavitation effect on diesel injection primary breakup has been reported in [9]. In GDi, detailed analysis of vortex structures in the nozzle flow and its effect on atomization might have been first reported in [10]. String cavitation induced by vortex flow was visualized by [11]. High fidelity LES analysis of cavitation in GDi nozzle replicas and validation using transparent nozzle visualizations were presented in [12]. A detailed analysis of the vortex dynamics induced surface dynamics in primary atomization using high fidelity simulation was presented in [13]. The present research is a direct extension of previous analysis of vortex driven atomization in diesel injection [1] [2] [3] contributed by the authors research group and provides new understandings on GDi atomization mechanism.

Material and Methods

The CLSVOF-LES methodology developed for diesel injection primary breakup analysis using an incompressible flow model[3][4][5] provided a starting point for this study. Several extensions were made to consider compressibility, cavitation and to enhance the interface scale resolution for the near-nozzle spray by introducing the Adaptive Mesh Refinement (AMR) technique. The details are described as follows.

A compressible two-phase three-component (n-heptane liquid, vapour and air) homogeneous mixture model, where all phases share the same velocity and pressure field, was adopted for the description of the flow system. The flow was assumed to be isothermal. The governing equations, consisting of the continuity and momentum equations for the mixture, the mass conservation equation for the air together with a volume of fraction constraint equation, and the level set function, are given below,

$$\frac{\partial \rho}{\partial t} + \nabla \cdot (\rho \vec{u}) = 0 \tag{1}$$

$$\frac{\partial (\rho \vec{u})}{\partial t} + \nabla \cdot (\rho \vec{u}\vec{u}) = -\nabla p + \nabla \cdot \bar{\bar{\sigma}} \tag{2}$$

$$\frac{\partial (\rho_{air} \alpha_{air})}{\partial t} + \nabla \cdot (\rho_{air} \alpha_{air} \vec{u}) = 0 \tag{3}$$

$$\frac{\partial f}{\partial t} + \nabla \cdot (\rho \vec{u} f) = 0 \tag{4}$$

where $\vec{\boldsymbol{u}}$ is the velocity vector, $\bar{\bar{\sigma}}$ the instantaneous viscous stress term, and f the level set function for the interface tracking. The mixture density $\boldsymbol{\rho}$ is calculated from a linear mixing law based on the corresponding volume fraction of air and fuel in a control volume, $\rho =$

$\alpha_{air}\rho_{air}+\alpha_{fuel}\rho_{fuel}$. The same applies for the mixture viscosity. In addition, the volume constraint condition $\alpha_{fuel} + \alpha_{air} = 1$ is enforced in each cell.

The cavitation phenomenon was modelled by introducing an Equation of State (EoS) for a barotropic fluid, where the fuel density is represented using a piecewise function of pressure. The transition between liquid and vapor state is determined by the saturation vapor pressure and the local pressure. A detailed description of the model formulation and examples of successful prediction of cavitation erosion in a GDi nozzle operated with E100 fuel are presented in [4]. According to [14], a Barotropic cavitation model produces correct bubble collapse speed in vapor condensation. This feature is important for the present study for the role of cavitation in the spray formation process.

An 1/6-sector model of an axial symmetric 6-hole nozzle together with a discharge volume 4mm x 4mm x 7mm was designed for the numerical investigation. To properly resolve large turbulence scales in the nozzle flow, high resolution hexahedral LES mesh was designed based on the estimation of the Taylor microscales (~2.4 um). The computational domain, boundary conditions and the nozzle part mesh are demonstrated in Figure 1. Wall refinement was applied to reach an average wall resolution y+ of about 1. The Wall Adapting Local Eddy Viscosity (WALE) model [15] was chosen for the sub-grid scale turbulent dissipation modelling.

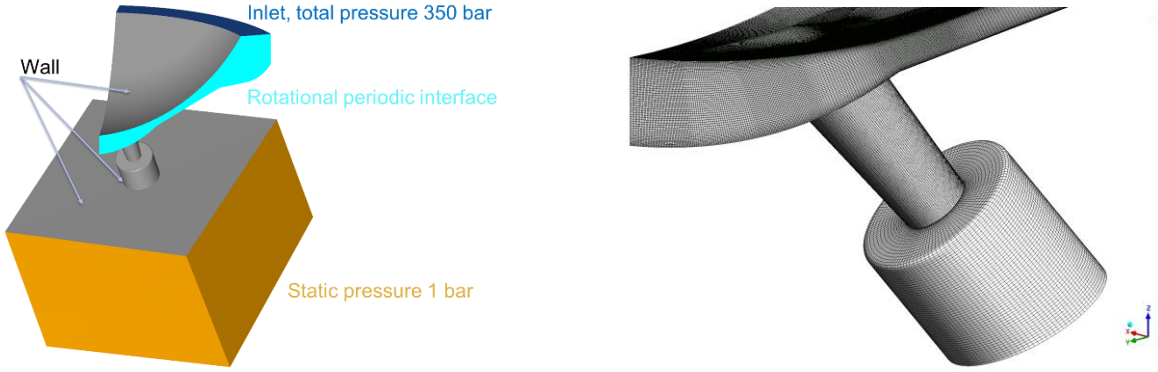

Figure 1**.** Computational domain and nozzle LES mesh

An implicit VOF formulation with compressive scheme, which is based on a second-order reconstruction method with a slope limiter of 2 [16], was used to track the fuel-air interface. A second-order bounded central differencing scheme was employed for the momentum equation, a body-force-weighted scheme was adopted for pressure interpolation and a first-order accurate upwind scheme for density advection together with a 1st-order implicit-in-time scheme to ensure numerical stability. A coupled pressure-velocity solver was applied and a time-step of 5e-9s corresponding to CFL <1. An AMR technique was applied to the spray region to have a good resolution of gas-liquid interfaces. A base mesh of 64μm was used with successive levels of refinement down to a minimum size of 4μm. The mesh adaption was made based on the normalised liquid volume fraction gradients referring to the global max value (refinement for a normalised value above 0.04 and coarsening for a value below 0.01) and the sub-grid viscosity ratio (refining for values above 5). This ensures a consistent resolution for the multi-scale turbulent and multi-phase flow.

Results and Discussion

1. In-nozzle flow

A snapshot of the nozzle flow is presented in Figure 2. The streamlines (2a) indicate that 3 major types of flow turning phenomenon occur in the nozzle sac. The most significant is the

counter-rotating circumferential flow turning of the fuel from both sides of the spray hole. Second is the seat flow turning of the fuel coming direct from the upstream of the spray hole location. The third is the turning of the fuel from the sac centre before entering the spray hole. Simultaneously the fuel gets accelerated in the process of flowing into the spray hole. Both the flow turning (streamline line curvature) and velocity acceleration promote vortex generation.

The corresponding instant vortex structure is presented in Figure 2b together with the shear stress contour on the needle surface. Two counter-rotating tornado-like large vortex pair linked to circumferential flow turning (type 1) are dominant while vortices linked to seat and sac flow turning (type 2, 3) can also be recognized. Both large vortices are directly attached to the needle surface and induce cavitation streams which also touch the needle. The shear stress contour on the needle surface provide an indicator of vortex intensity on the wall. Time sequences of vortex structures and vapor iso-surface at a time interval of 5e-6s are demonstrated in Figure 3, indicating highly transient behaviour. The two counter-rotating vortices wobble with high speeds in the sac, the intensity of each counterpart alternates by turns. One vortex detaches from the needle once its intensity becomes weaker and gets attached again when the intensity rises. The vortex wobbling and intensity alternation by turns lead to changes of cavitation appearance. It is observed in most of the recorded flow visualizations that large scale vortices and cavitation streams survive until the spray hole outlet. This is due to two reasons. One is that a convergent spray hole as here is good to maintain vortex intensity or slow down vortex decays compared to other hole shapes. Another is that the spray hole in a GDi nozzle is too short for the large scales to break down completely

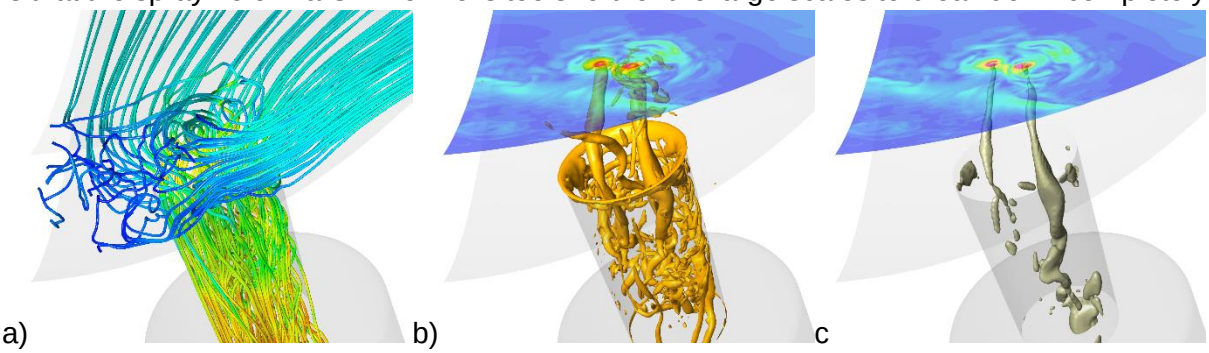

Figure 2. a) Instant streamline, b) vortex (Q=9e13 [1/s2]) (middle), c) cavitation (vapor VOF0.1); Needle wall coloured by wall shear.

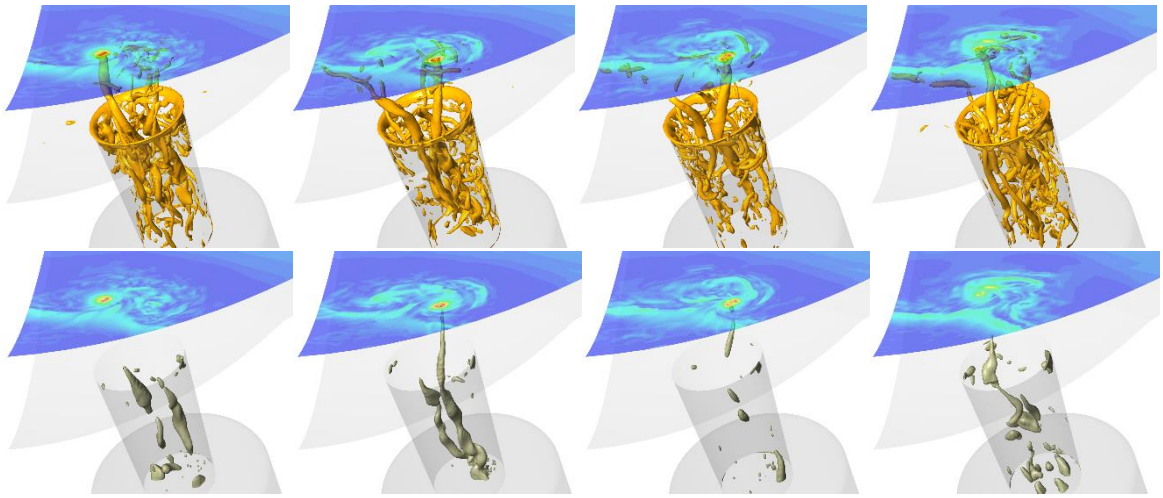

Figure 3. Sequences of vortex (Q=9e13 [1/s2]) and cavitation (vapor VOF0.1) at a time interval 5e-6 s.

into small scales. These large vortices (secondary flow) are expected to contain high energies. This is confirmed by the instantaneous turbulent energy contour, calculated using $\frac{1}{2}\rho(\vec{u}-\overrightarrow{u_0}).(\vec{u}-\overrightarrow{u_0})$ where $\overrightarrow{u_0}$ is the time average local velocity, and the time averaged turbulent energy contour demonstrated in Figure 5. For an injection pressure of 350bar, the local max of the instant turbulence energy reaches 125bar while the max value for the time average is about 20bar. The high instant values is due to the flow transience of those large scale vortices (intermittency) while the time averaged values represent the energy of small scale turbulence. Therefore, these large-scale vortices (secondary flow) are expected to play a more significant role in the initial stage of GDi spray formation than the small-scale turbulence.

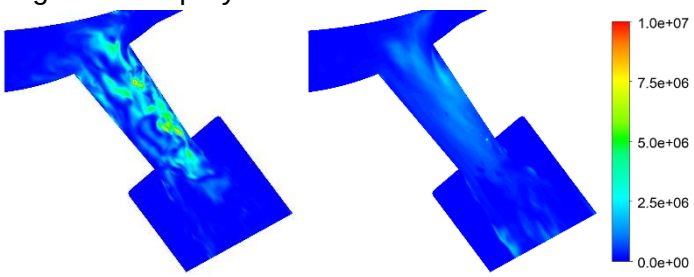

Figure 4. Instant and time averaged turbulence kinetic energy [bar] defined by $\frac{1}{2}\rho(\vec{u}-\overrightarrow{u_0}).(\vec{u}-\overrightarrow{u_0})$.

2. Vortex and Cavitation driven atomization

A zoomed view of liquid atomization process in the counter bore (the larger step hole) and near-nozzle region is presented in Figure 5. Inside the spray hole, the rotating kinetic motions of the vortices are confined by the convergent spray hole wall. Cavitation is supressed for the same reason. Once the fuel leaves the spray hole and enters the counter bore, this confinement is removed. Then the vortices (secondary flow) expand immediately, which leads to massive cavitation inside the liquid core. The massive cavitation and fuel expansion effectively destroy the liquid core, turn it into thin film like structures and ligaments. Hence primary breakup in GDi is majorly triggered by vortex and cavitation. Increasing injection pressure leads to increased cavitation inside a counter bore, enhanced liquid fragmentation and higher wall shear for the cleaning of coking on the counter bore wall as has been reported in [17]. In addition, it is noticed that the atomization is more intensified on the seat side (top side of spray hole) than the sac side (bottom side). This can be understood by referring to the vortices. On the seat side of the spray hole there are much more smaller vortices caused by the seat flow turning than the sac side. These small vortices produce the intensified liquid atomization on the top side of the spray.

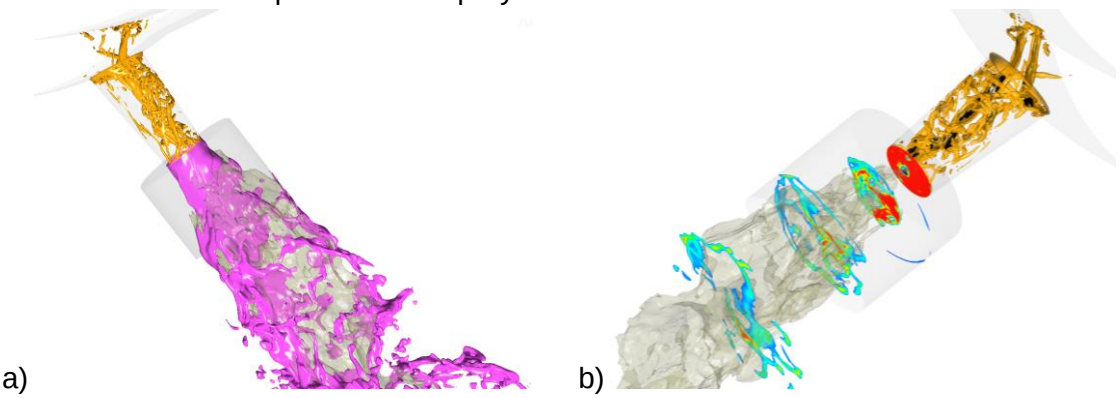

Figure 5. Vortex and cavitation driven atomization, yellow: vortex, iso-surface Q=9e13 [1/s^2]; magenta: liquid, iso-surface volume fraction = 0.5; grey: vapor, iso-surface volume fraction = 0.5; black: vapor, iso-surface volume fraction = 0.1; planes: liquid volume fraction contours.

The flow is highly transient, cavitation vapor extends from 0.5 to 1 mm outside of the nozzle before getting collapsed. The cross-section view of near-nozzle spray for the same time sequences as in Figure 4 are demonstrate in Figure 6. All events indicate that liquid core get destroyed when the fuel reaches the counter bore outlet and show typical hollow spray structures.

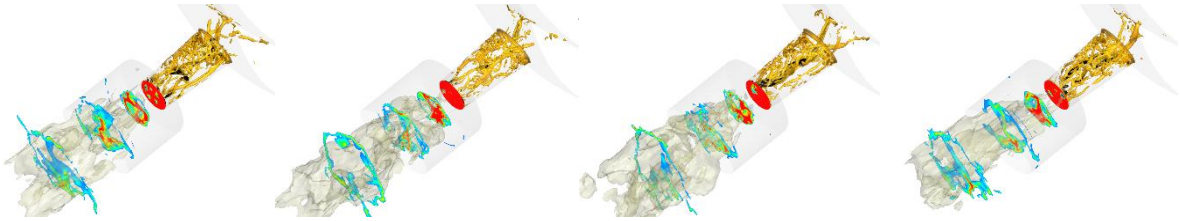

Figure 6**.** Sequences of vortex and cavitation driven atomization events at a time interval 5e-6 s

3. Implication for spray control and spray modelling

The above qualitative results demonstrate the effect of vortex and cavitation on the primary breakup of liquid fuel in GDi. Understanding derived from the present study can have implications on spray control and on GDi spray modelling. Spray control knowledge development is so far empirical. The present results suggest that using nozzle design geometry to control vortices and cavitation can be an effective approach to realize knowledge guided spray control. An example was reported in [18] that specific needle geometric features can be introduced to control the flow separation and vortex shedding from the needle and through which to control the spray stability and penetration. The present results provide a consolidated background to that previous work.

The large-scale vortices (intermittency) contain higher energy than small-scale turbulence and are highly transient and depend on nozzle design. Their effect has not yet been considered in many widely applied primary breakup models. Therefore, from the spray modelling point of view, a nozzle flow coupled simulation approach is essential. A modelling approach taking into account of the specific flow structures and transience of each individual nozzle will significantly improve the spray prediction capability and potentially reach a universality for all different nozzle designs. Based on this understanding, the authors group has developed a VOF coupling spray simulation approach. The prediction capability has been confirmed by using test data (spray images, penetration, and targeting) for more than 20 different nozzles from real applications including various spray patterns and extremely contrasting design geometries. The need of model calibration effort is also significantly reduced. The results are going to be reported in another publication.

4. Transfer function for spray correlation

On the basis of the analysis of vortex driven atomization [1] [2][10], transfer functions (metrics), which is derived from URANS nozzle flow simulation, have been developed for spray correlation. The concept is outlined in Figure 7. Local coordinates systems (LCS) are defined at counter bore outlet with an axis aligned with the spray hole axis. The ensemble average of the LCS velocity components and their corresponding kinetic energy are calculated at the outlets of a spray hole and counter bore. Taking the hypothesis that the kinetic energy of the axial velocity component (AKE) promotes spray penetration (named as penetration energy) while both the secondary flow kinetic energy ($NAKE$) and the turbulence kinetic energy (TKE) promote atomization and dispersion (their sum named as atomization energy ATE). It is generally observed that $NAKE$ is much higher than TKE. This is consistent with the LES findings (refer to Figure 5) that the large-scale vortices (intermittency) contain more kinetic

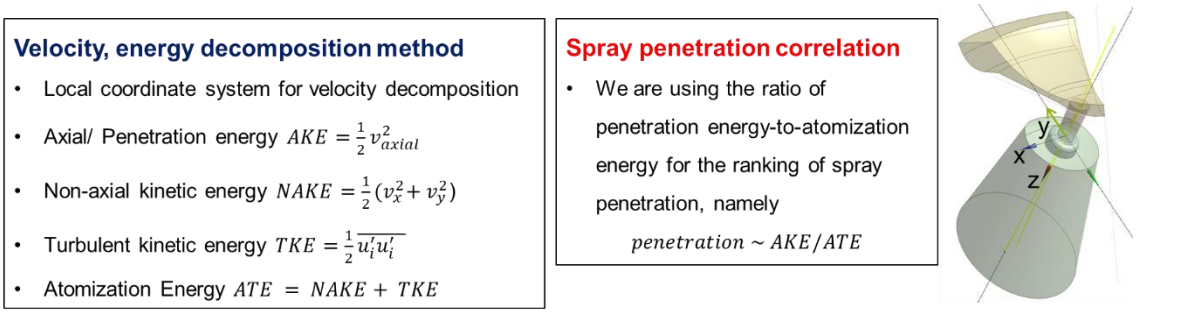

Figure 7. Definition of spray correlation transfer function based on URANS nozzle flow simulation.

Figure 8. Spray penetration correlation using transfer function based on URANS simulation: a) Two extreme contrast parts with the same design, b) Results from a counter bore size impact study.

energies than turbulence. The quantity AKE/ATE has been found to have a good correlation to the measured spray penetration. Two examples are presented in Figure 8. Example a) shows spray images at 1.2ms after start of injection for two contrast injector parts of the same design. The measured spray penetration is dominated by the middle jet from the spray hole 1, whose axis is parallel to the injector axis (low flow turning). The penetrations of the BOB and the WOW part were measured to be 62 mm and 91 mm, respectively. Their ratio is found to be close to the ratio of the corresponding AKE/ATE values calculated at the hole 1 counter bore outlet, 33 : 62. Example b) presents results from a study about the effect of counter bore diameter on spray penetration. URANS simulations were carried out for a 60-degree nozzle sector model (6-hole nozzle) with varying counter bore diameters and lengths (keeping the rest geometry the same). Some simulation cases were repeated using measured geometry. The concept of opening angle has been introduced to characterize the counter bore diameter and length effect, which corresponds to the geometric restriction angle from spray hole outlet to counter bore outlet (Figure 8b). Values of AKE/ATE at the counter bore outlet and the values of measured spray penetration (in injector axis direction) at 1.2 ms after start of injection are plotted together as functions of the counter bore opening angle. The behaviour of both quantities show a very similar trend. The measured spray penetration reduces with increasing counter bore opening angle, but remains almost unchanged when the opening angle goes above 40 degree. It is worth pointing out that the spray measurement data were obtained almost one year later than the CFD simulation. This suggests a good prediction capability of this transfer function (metrics) using AKE/ATE to correlate to the nozzle flow simulation, design geometry to the measured spray penetration. Further analysis of transfer functions using 15 real nozzle data are summarized in a Master thesis report [19]. It is worth mentioning that the transfer function based correlation approach has even been found to have a better prediction capability for the relative spray penetration for two different nozzle designs than a DPM spray simulation without adopting a nozzle flow coupled simulation approach.

Conclusions

Detailed analysis of vortex structures, cavitation in a GDi nozzle and their effect on spray formation has been carried out using the CLSVOF-LES method. The results illustrate the vortex and cavitation driven atomization phenomenon. The following understanding has been obtained:

- A highly transient large-scale counter-rotating vortex pair dominates the flow dynamics and cavitation in a spray hole. These large-scale vortices cannot completely break down into small scales due to the short spray hole length in a GDi nozzle. They contain much higher energy than the small-scale turbulence.
- The liquid fragmentation starts in the counter bore. The vortices trigger fuel expansion and massive cavitation in the counter bore, which breaks the liquid fuel into hollow structures and ligaments.

The above understanding provides a potential effective idea for knowledge based spray control via vortex control and explains the theoretical background why a nozzle flow coupled approach is needed for GDi spray simulation. In addition, a transfer function for spray penetration correlation is presented.

Acknowledgments

The LES simulation was realized in the PhD project of Eduardo Gomez Santos in 2018. Post-processing was made by Ramesh Venkatasubramanian. The European Union Horizon-2020 Research and Innovation Program funding to the PhD project of Eduardo Gomez Santos (No 675676), the Luxembourg FNR funding to the PhD project of Ramesh Venkatasubramanian (No 12553319), the HPC research license grant from ANSYS and the CPU time granted by Gompute are gratefully acknowledged.

References

[1] Shi J, Aguado Lopez P, Gomez Santos E, Guerrassi N, Dober G, Bauer W, Lai M-C, Wang J, *28th European conference on Liquid Atomization and Spray Systems*, Valencia, 2017

[2] Shi J, Lopez Aguado P, Guerrassi N, Dober, G, *MTZ Worldwide*, 2017

[3] Shi J, Aguado Lopez P, Gomez Santos E, Guerrassi N, Dober G, Bauer W, Lai M-C, Wang J, 14th International Conference on Liquid Atomization and Spray Systems, Chicago, 2018.

[4] Gomez Santos E, Shi J, Venkatasubramanian R, Hoffmann G, Gavaises M, Bauer W, Fuel, 2021

[5] Piock W, Hoffmann G, Gomot B, Dober G, Spakowski J, Heusler H, 40. Internationales Wiener Motorensymposium, Wien, 2019

[6] Andriotis A, Gavaises M, Arcoumanis C, Journal of Fluid Mechanics, 2008

[7] Andriotis A, Gavaises M, Atomization and Sprays, 2009

[8] Guan W, He Z, Zhang L, Guo G, Cao T, Leng X, Fuel, 2021

[9] Blume M, Schwarz P, Rusche H, Weiß L, Wensing M, Skoda, R, Atomization and Sprays, 2019

[10] Shi J, Wenzlawski K, Helie J, Nuglisch H, Cousin J, 23rd Annual European Conference on Liquid Atomization and Spray Systems, Borno, 2010

[11] Mamaikin D, Knorsch T, Rogler P, Wensing M, Atomization and Sprays, 2019

[12] Piscaglia F, Giussani F, Hèlie J, Lamarque N, Aithal SM, Int. J. of Multiphase Flow, 2021

[13] Zandian A, Sirignano W, Hussain F, Journal of Fluid Mechanics, 2018.

[14] Koukouvinis P, Gavaises M, Li J, Wang L, Fuel, 2016.

[15] Nicoud F, Ducros F, Flow, Turbul Combust, 1999.

[16] Ansys Fluent Theory Guide, 2019.

[17] Shi J, Gomez Santos E, Hoffman G, Dober G, MTZ Worldwide, 2018.

[18]Shi J, Patent WO2012143264A1, 2012.

[19] A. Mieuguem, Delphi Technologies Master Thesis Report, Bascharage, 2018.